The Generalized TLM-Based FDTD—Summary of Recent Progress

Zhizhang Chen, *Senior Member, IEEE*, and Jian Xu

***Abstract*— The transmission-line-matrix (TLM)-based finite-difference time-domain (FDTD) method has been generalized recently to incorporate graded mesh and anisotropic media. The method is equivalent to the three-dimensional TLM symmetrical condensed node, but is formulated and computed in a FDTD fashion. Therefore, it retains certain features of both the TLM and FDTD methods. This letter reports recent progress in modeling with the TLM-based FDTD method, namely, successful implementation of the perfectly matched layer (PML) and simulation of nonlinear wave propagation.**

I. Introduction

TWO WIDELY employed time-domain numerical techniques are the finite-difference time-domain (FDTD) method initially formulated by Yee [1] and the transmission-line-matrix (TLM) method proposed by Johns [2]. The two methods have their respective advantages and disadvantages. The FDTD method is easily understood and implemented as it is a direct approximation of the Maxwell's equations, while the TLM requires transforms of field quantities to circuit parameters to obtain an appropriate scattering matrix. Although the transforms are not complicate in most cases, they are sometimes not easily understood and implemented. For example, the recently proposed perfectly matched layer (PML) absorbing scheme has been successfully applied with the conventional FDTD of Yee's scheme [3], but not yet in a TLM algorithm due to the difficulties in obtaining an appropriate scattering matrix. On the other hand, TLM enjoys less numerical dispersion [4] and easy uses of many circuit and network concepts and, most significantly, the condensation of all the field components at a node. In application to anisotropic media with nonzero off-diagonal elements in permittivity tensors, TLM can be directly employed [5], while the conventional FDTD can be applied only after introduction of additional averaging schemes at every node [6].

In spite of these differences and the fact that the two methods were developed independently, they have been demonstrated to be equivalent under certain conditions. In the case of the three-dimensional (3-D) TLM symmetrical condensed node (SCN), initial work was reported in [7] and a further generalization was presented in [8].

To exploit the equivalence between the TLM method and the FDTD method, a TLM-based FDTD was proposed [7] and further generalized recently [9]. The method is equivalent to the 3-D TLM SCN, but is formulated and computed in a FDTD fashion directly in terms of field quantities. As a result, it retains features of both the TLM and FDTD methods and allows direct use of modeling techniques already developed for the TLM method and the conventional FDTD of Yee's scheme. It is in this regard that this letter reports our recent research results, namely, the implementation of PML and the incorporation of nonlinearity in the TLM-based FDTD.

Manuscript received July 30, 1996. This work was supported by the Natural Science and Engineering Research Council of Canada.

The authors are with the Department of Electrical Engineering, Technical University of Nova Scotia, Halifax, Nova Scotia, B3J 2X4 Canada .

Publisher Item Identifier S 1051-8207(97)00508-4.

II. The Generalized TLM-Based FDTD Formulation

Details about the TLM-based FDTD formulation can be found in [7] and [9]. Only a brief description is given here.

For a numerical solution, problem space and time of interest need to be discretized. Space is usually discretized into many 3-D cells with dimension $\delta x \times \delta y \times \delta z$. In contrast to Yee's scheme [1], the TLM-based FDTD scheme defines the field vectors in a "condensed" manner [7]. At the center of a 3-D cell, all six field components of $\boldsymbol{E}$ and $\boldsymbol{H}$, and their corresponding flux densities, $\boldsymbol{D}$ and $\boldsymbol{B}$, are defined. At the grid point on the boundary surfaces of the 3-D cell, only the field components tangential to the surface are considered. As a result, the E- and H-field components are not separated in space and are continuous across the interface of the two adjacent cells.

To update the field components at the center of the 3-D cell, Maxwell's equations are finite-differenced in respect to the center. For example, for D_x, one can obtain

$$\begin{aligned}&\frac{D_x^n(i,j,k)-D_x^{n-1}(i,j,k)}{\delta t}\\&\quad+\sigma_{ex}\frac{E_x^n(i,j,k)+E_x^{n-1}(i,j,k)}{2}\\&=-\frac{H_y^{n(1/2)}(i,j,k+\frac{1}{2})-H_y^{n-(1/2)}(i,j,k-\frac{1}{2})}{\delta z}\\&\quad+\frac{H_z^{n-(1/2)}(i,j+\frac{1}{2},k)-H_z^{n-(1/2)}(i,j-\frac{1}{2},k)}{\delta y}.\end{aligned}\tag{1}$$

With the medium constitutive relationships shown in the following, one can then compute the field components at the center of a 3-D cell

$$\boldsymbol{D}=\boldsymbol{D}(\boldsymbol{E},\boldsymbol{H})\tag{2}$$

$$\boldsymbol{B}=\boldsymbol{B}(\boldsymbol{E},\boldsymbol{H}).\tag{3}$$

To update the field components at the boundary surfaces of the 3-D cell, a special TLM-based averaging process is applied. The details can be found in [7] and [9].

III. Implementation of PML in the TLM-Based FDTD Scheme

The recently proposed PML scheme presents a very effective absorbing boundary for FDTD-based analysis of electromagnetic problems [3]. Further enhancement for absorption of evanescent modes has led to the development of the modified PML (MPML) scheme in two dimensions [10]. The MPML boundaries in two dimensions were shown being placed closer to scatters than the original PML.

MPML can be expanded to three dimensions in a similar way described in [10]. For example, one can obtain

$$\mu_0\mu_z\frac{\partial H_{yz}}{\partial t}+\sigma_z^* H_{yz}=-\frac{\partial E_x}{\partial z} \tag{4}$$

$$\epsilon_0\epsilon_z\frac{\partial E_{xz}}{\partial t}+\sigma_z E_{xz}=-\frac{\partial H_y}{\partial z}. \tag{5}$$

The equations for the other split components can also be obtained without much difficulty.

The matched conditions can be found as follows:

$$\frac{\sigma_x}{\epsilon_0}=\frac{\sigma_x^*}{\mu_0},\quad \frac{\sigma_y}{\epsilon_0}=\frac{\sigma_y^*}{\mu_0},\quad \frac{\sigma_z}{\epsilon_0}=\frac{\sigma_z^*}{\mu_0} \tag{6}$$

$$\epsilon_x=\mu_x,\quad \epsilon_y=\mu_y,\quad \epsilon_z=\mu_z. \tag{7}$$

Here, additional permittivities, $\epsilon_x, \mu_x, \epsilon_y, \mu_y, \epsilon_z$, and μ_z are introduced in a MPML region to control the absorption of evanescent energy.

In order to achieve minimal numerical reflections, electric loss and permittivity spatial profiles need to be chosen carefully. For example, as shown in [10], one can use

$$\sigma_z=\sigma_z^{\max}\left(\frac{\rho}{\delta}\right)^2,\quad \epsilon_z=1+\epsilon_z^{\max}\left(\frac{\rho}{\delta}\right)^2. \tag{8}$$

Implementation of the MPML scheme in the TLM-based FDTD grid is straightforward. Only the field components at the center of a 3-D cell need to be split and computed by finite-differencing (4) and (5); the field components at the boundary surfaces need not. They are still computed via the averaging procedure, which is not affected by the requirements of split of field components in a PML region.

To test the validity of the MPML in the TLM-based FDTD grid, a section of WR28 waveguide with both ends terminated with MPML layers was chosen. The choice was made because waves inside a rectangular waveguide can be considered as superposition of many plane waves with different incident angles, each associated with different operating frequency. In addition, evanescent modes can be clearly identified by selecting the operating frequency points below the cutoff frequency. This allows a numerical evaluation of the overall performance of the MPML.

The waveguide has a dimension of 7.112 mm × 3.556 mm. The waveguide is discretized into $14\Delta l$ in height, $28\Delta l$ in width and $60\Delta l$ in length. The maximum of electric loss $\sigma_z^{\max}$ of the MPML was chosen to be 1.24, and the maximum dielectric constant $\epsilon_z^{\max}+1$ was chosen to be five.

Fig. 1 shows the return loss obtained numerically for TE_{31} mode. As can be seen, good absorption is achieved over the operating band with return loss below −50 dB. Even for the evanescent modes, less than −20 dB of return loss is found when 16 MPML's were used.

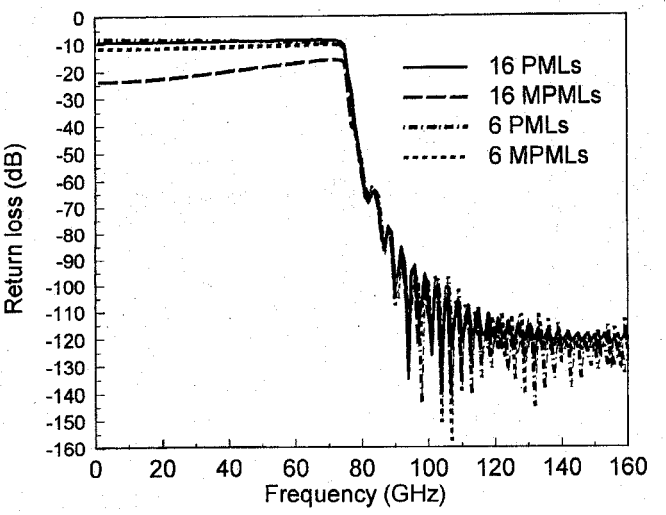

Fig. 1. Return loss for TE_{31} mode in the WR28 waveguide. The theoretical cutoff frequency is 76.0 GHz.

IV. Modeling of Nonlinear Media

To treat the nonlinearity of a medium, the Z-transform technique is applied. Details of the transform can be found in [11]. Here, only the final results are given.

For a medium with linear dispersion and nonlinear polarization with Kerr and Raman effects, the relation between $\boldsymbol{D}$ and $\boldsymbol{E}$ can be found as

$$E^n=\frac{\frac{1}{\epsilon_s}D^n-S_L^{n-1}+\chi_0^{(3)}\cdot\alpha\cdot[2\cdot(E^{n-1})^3]}{\epsilon_\infty+\chi_0^{(3)}(1-\alpha)\cdot S_R^{n-1}+\chi_0^{(3)}\cdot\alpha\cdot 3\cdot(E^{n-1})^2} \tag{9}$$

where

$$S_L^{n-1}=c1\cdot S_L^{n-2}-c2\cdot S_L^{n-3}+c3\cdot E^{n-1}$$

$$S_R^{n-1}=cnl1\cdot S_L^{n-2}-cnl2\cdot S_L^{n-3}+cnl3\cdot(E^{n-1})^2.$$

Here $c1, c2, c3, cnl1, cnl2$, and $cnl3$ are the constants that define the linear dispersive and nonlinear effects of a medium. Values for them can be found in [11].

The above equation constitutes a recursive formula for the constitutive relationship (2) and (3) in an 2explicit form. It permits updating of electric field $\boldsymbol{E}$ at the center of a 3-D cell directly from electric flux density $\boldsymbol{D}$ with (1). The averaging process again remain unaffected.

A soliton propagation in the dispersive nonlinear optical medium is simulated. In order to effect the comparison, the geometry and parameters were taken to be the same as those in [11] for silica glass. Fig. 2 shows the time-domain graph of the pulse at three different time steps. The simulation was done in a one-dimensional problem space of 25 000 cells. As can been seen, after some distance of propagation, the initial pulse settled into a soliton. The result agrees well with that presented in [11]. Fig. 3 shows the peak-to-peak amplitudes of the pulse in frequency domain at different locations. The frequency-domain solution shows a decided shift as expected.

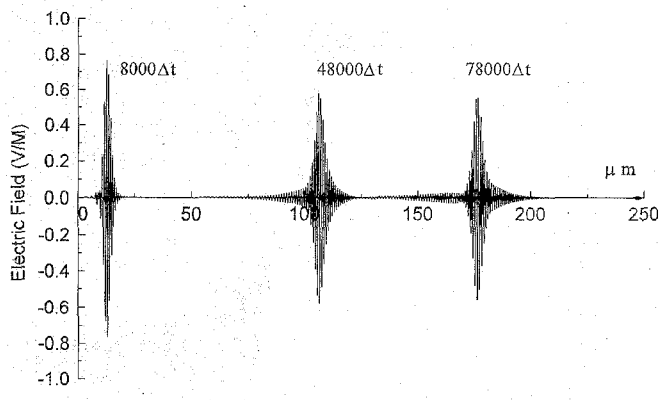

Fig. 2. Electric field propagation with initial amplitude of 1.0 V/m. The soliton is formed at about 100 μm.

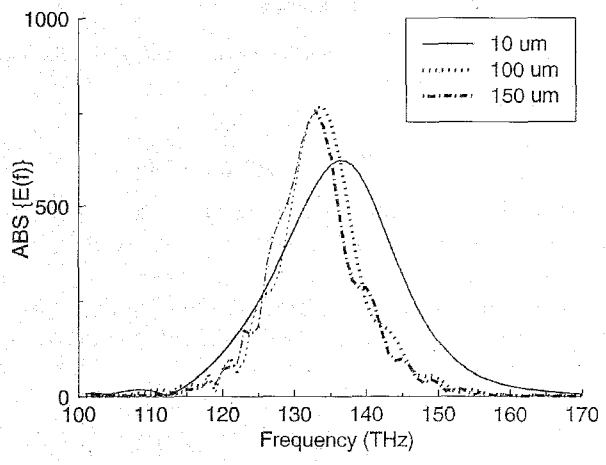

Fig. 3. Peak-to-peak amplitudes of the electric field in frequency domain at different locations.

V. Conclusion

In this letter, a summary has been presented of recent progress in the implementation of PML and modeling of nonlinear media with the TLM-based FDTD method. The numerical results show that by employing modeling techniques already developed for the conventional FDTD, the TLM-based FDTD technique can now be used to solve open structure and nonlinear dispersive medium problems.

Acknowledgment

The authors would like to thank J. A. Yurchesyn of Nova Scotia Power, Canada, for correcting grammatical errors in this manuscript.

References

[1] K. S. Yee, "Numerical solution of initial boundary value problems involving Maxwell's equations," *IEEE Trans. Antennas Propagat.*, vol. AP-14, no. 3, pp. 302–307, May 1966.

[2] P. B. Johns, "A symmetrical condensed node for the TLM method," *IEEE Trans. Microwave Theory Tech.*, vol. MTT-35, no. 4, pp. 370–377, Apr., 1987.

[3] J. P. Berenger, "A perfectly matched layer for the absorption of electromagnetic waves," *J. Comput. Phys.*, pp. 185–200, Oct.1994.

[4] K. L. Shlager, J. G. Maloney, S. L. Ray, and A. P. Peterson, "Relative accuracy of several finite-difference time-domain methods in two and three dimensions," *IEEE Trans. Antennas Propagat.*, vol. 41, no. 12, pp. 1732–1736, Dec. 1993

[5] J. Huang and K. Wu, "A unified TLM model for wave propagation of electrical and optical structures considering permittivity and permeability tensors," *IEEE Trans. Microwave Theory Tech.*, vol. 43, no. 10, pp. 2472–2477, Oct. 1995.

[6] J. Schneider and S. Hudson, "The finite-different time-domain method applied anisotropic material," *IEEE Trans. Antennas Propagat.*, vol. 41, no. 7, pp. 994–1000, July 1993.

[7] Z. Chen, M. M. Ney, and W. J. R. Hoefer, "A new finite-difference time-domain formulation and its equivalence with the TLM symmetrical condensed node," *IEEE Trans. Microwave Theory Tech.*, vol. 39, no. 12, pp. 2160–2169, Dec. 1991.

[8] J. Hang and R. Vahldieck, "Direct derivation of TLM symmetrical condensed node and hybrid symmetrical condensed node from Maxwell's equations using centered differencing and averaging," *IEEE Trans. Microwave Theory Tech.*, vol. 42, no. 12, pp. 2554–2561, Dec. 1994.

[9] Z. Chen, "The generalized TLM based finite-difference time-domain method and its applications to frequency-dependent and anisotropic media," in *Dig. 1996 IEEE Int. Microwave Symp.*, San Francisico, June 17–21, pp. 435–438, 1996.

[10] B. Chen, D. G. Fang, and B. H. Zhou, "Modified Berenger PML absorbing boundary condition for FD-TD meshes," *IEEE Microwave Guided Wave Lett.*, vol. 5, pp. 399–401, Nov 1995.

[11] D. Sullivan, "Nonlinear FDTD formulation using transforms," *IEEE Trans. Microwave Theory Tech.*, vol. 43, no. 3, pp. 676–682, Mar. 1995.